applied sciences

MDPI

Article

Field Reconnaissance and Earthquake Vulnerability of the RC Buildings in Adıyaman during 2023 Türkiye Earthquakes

Ercan Işık [1], Fatih Avcil [1], Rabia İzol [2,*], Aydın Büyüksaraç [3], Hüseyin Bilgin [4], Ehsan Harirchian [5,*] and Enes Arkan [6]

[1] Department of Civil Engineering, Bitlis Eren University, Bitlis 13100, Türkiye; eisik@beu.edu.tr (E.I.); favcil@beu.edu.tr (F.A.)
[2] Department of Civil Engineering, Faculty of Engineering Middle East Technical University, Ankara 06410, Türkiye
[3] Çan Vocational School, Çanakkale Onsekiz Mart University, Çanakkale 17400, Türkiye; absarac@comu.edu.tr
[4] Department of Civil Engineering, Epoka University, 1001 Tirana, Albania; hbilgin@epoka.edu.al
[5] Institute of Structural Mechanics (ISM), Bauhaus-Universität Weimar, 99423 Weimar, Germany
[6] Department of Architecture, Bitlis Eren University, Bitlis 13100, Türkiye; earkan@beu.edu.tr
* Correspondence: rizol@metu.edu.tr (R.İ.); ehsan.harirchian@uni-weimar.de (E.H.)

Abstract: The 6th February 2023 Pazarcık and Elbistan earthquakes (M_w = 7.7 and M_w = 7.6) caused great destruction in many cities and were the disaster of the century for Türkiye. The greatest destruction was caused in the provinces of Hatay, Kahramanmaraş, and Adıyaman during these earthquakes, which were independent of each other and occurred on the same day. Information about earthquakes and strong ground motion records is given within the scope of this study. Reinforced concrete (RC) structures which constitute a large part of the urban building stock in the earthquake region were exposed to structural damage at different levels. The structural damage in the RC structures in the city center, Gölbaşı, and Kahta districts of the province of Adıyaman was evaluated within the scope of earthquake and civil engineering after field investigations. Insufficient RC, low-strength concrete reinforcement problems, RC frame failure, heavy overhang, short columns, soft story, and pounding effect are the main causes of the earthquake damage. The presence of these factors that reduce the earthquake resistance of RC structures increased the damage level. In addition, the fact that the earthquakes occurred nine hours apart and the continuation of aftershocks during that period negatively affected the damage levels. It has been observed that structures that receive the necessary engineering services during the construction and project phases ensure the safety of life and property, even if the structure is slightly damaged. In this study, we also tried to reveal whether the target displacements were satisfactorily represented by numerical analysis for a sample RC structure.

Keywords: Kahramanmaraş earthquakes; Adıyaman; field reconnaissance; RC buildings; damage

check for updates

Citation: Işık, E.; Avcil, F.; İzol, R.; Büyüksaraç, A.; Bilgin, H.; Harirchian, E.; Arkan, E. Field Reconnaissance and Earthquake Vulnerability of the RC Buildings in Adıyaman during 2023 Türkiye Earthquakes. *Appl. Sci.* **2024**, *14*, 2860. https://doi.org/10.3390/app14072860

Academic Editors: Bijan Samali and Amir M. Yousefi

Received: 28 February 2024
Revised: 22 March 2024
Accepted: 25 March 2024
Published: 28 March 2024

1. Introduction

Türkiye has experienced an enormous loss of life and property due to two major earthquakes centered in Kahramanmaraş, which occurred at intervals of nine hours. Earthquakes in the East Anatolian Fault Zone (EAFZ), which is one of Türkiye's main tectonic structures, caused very heavy damage in 11 different cities (Figure 1). The first earthquake occurred in Pazarcık, Kahramanmaraş (M_w = 7.7) on 6 February 2023 at 04:17 and lasted for approximately 75 s. The second earthquake occurred on the same day at 13:24 in Elbistan, Kahramanmaraş (M_w = 7.6) and lasted approximately 25 s. Following these earthquakes, more than 10,000 aftershocks have occurred as of 22 March 2023.

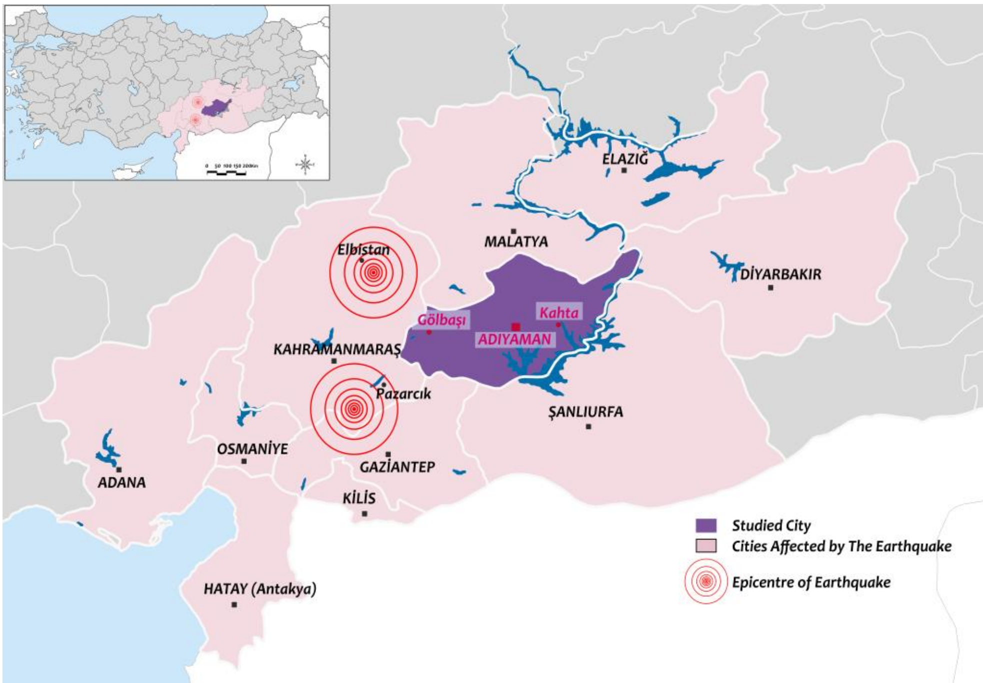

Figure 1. The affected provinces during the Kahramanmaraş earthquakes and representation of Adıyaman and studied districts.

The highest loss of life and property was observed in Adıyaman, Hatay, and Kahramanmaraş provinces. Within the scope of this paper, the cause–effect relationships of damage to RC structures in city center, Gölbaşı, and Kahta districts of Adıyaman were examined by the authors as a result of a detailed field investigation.

Buildings suffered extensive and widespread damage. Out of a total population of 85 million, it was predicted that the earthquake affected around 14 million individuals. Of those, 1.5 million became homeless, over 105,000 were injured, and over 50,000 were killed. The Turkish government published numbers showing that the cost of earthquake damage to private and state properties was USD 104 billion. Many structures, including RC, masonry, and historical buildings, suffered major damage or collapsed.

Determination of the structural damage after an earthquake is important for the continuation of social life, the realistic determination of the earthquake hazard of the settlements, and the development of regulations related to buildings. The collection of data regarding earthquake and civil engineering is important. Damage assessments at this stage should be carried out as quickly and practically as possible. In this work, observational evaluations were made [1–5]. Each of these and similar studies carried out or to be carried out after an earthquake is considered a case study and can significantly contribute to both practice and academia. Many publications examine the structural damage in reinforced concrete structures in different countries, such as Türkiye, due to the loss of life and property caused by disasters, within the framework of cause and effect. Alih et al. [6] reported their observations after the earthquake in Malaysia in 2015. They observed that most of the RC structures in the affected area suffered significant damage. They stated that the major reasons for the failure in reinforced concrete structures are the strong beam and weak column condition, the detailing of the structural components with non-ductile elements, short column effects, and soft–weak story mechanisms. Vlachakis et al. [7] studied the earthquake that caused severe damage with a magnitude of M_w = 6.3 which struck the SE of Lesvos Island on 12 June 2017. The study aims to present the models of structural damage and collapse caused by the Lesvos earthquake to masonry structures, highlighting the causes and weaknesses or the factors that prevent them. Jara et al. [8] investigated and evaluated the region after the earthquake that affected Mexico City on 19 September 2017. The observations showed that first soft-story buildings are the most common situation for collapsed buildings. They also proposed to analyze the seismic damage observed in the study, evaluate the seismic fragility of typical soft-story structures, and propose strengthening alternatives, including braces and energy distribution systems, to increase the seismic capacity of existing buildings. Yurdakul et al. [9] conducted field observations after the earthquake in the district of Sivrice of the province of Elazığ on 24 January 2020 and investigated the causes of losses and structural damage. The seismic damage observed in the structural and non-structural members of reinforced concrete structures after the earthquake has been reported. They concluded that the damage in the earthquake was mainly due to low material quality and a lack of control mechanisms during construction. Liu et al. [10] conducted in-depth research on the earthquake damage to various structures due to the M = 8.1 earthquake that occurred in Pokhara, Nepal, on 25 April 2015 and caused the death of thousands of people. They put forward strengthening measures and recommendations for post-earthquake reconstruction. Mertol et al. [11] presented their observations in reinforced concrete buildings after the earthquake near the district of Sivrice of the province of Elazığ on 24 January 2020. They suggested that almost all of the destroyed or heavily damaged reinforced concrete buildings were built between 1975 and 1998. Therefore, the buildings constructed between 1975 and 1998 in the region should be structurally re-evaluated to prevent loss of life and property in future earthquakes. Bayrak et al. [12] presented their field investigations and evaluations after the earthquake in the district of Sivrice of Elazığ on 24 January 2020. The collapse mechanisms of the structures were studied, and the causes of the damage were stated. Dogan et al. [13] studied masonry and rural structures as well as reinforced concrete buildings damaged in the Sivrice, Elazığ earthquake on 24 January 2020. They also compared the causes of damage and collapse observed in buildings with previous damage in Türkiye. Sayın et al. [14] summarized the earthquake region's past and present seismic characteristics after 24 January 2020 regarding the Sivrice, Elazığ (Mw = 6.8) earthquake. As a result of the observations, the damage is classified as occurring to reinforced concrete structures, masonry houses, and non-residential structures, and the lessons to be learned are stated. Caglar et al. [15] examined different types of structural damage observed after the earthquake. Many structural inadequacies, such as inadequate earthquake-resistant construction techniques, low concrete quality, and poor workmanship, have been cited as the main causes of damage. Gurbuz et al. [16], after the earthquake that occurred off the Aegean Sea on 30 October 2020 and which also affected İzmir, studied the effect of the earthquake on the structures in the region through field investigations. Some preliminary analyses were conducted to study the causes of the observed seismic damage on reinforced concrete buildings. In addition, many studies have been conducted around the world investigating the seismic effects of earthquakes and the damage to structures after earthquakes [17–23].

After the Kahramanmaraş earthquakes, which were the disaster of the century for Türkiye, studies about the evaluation of structural damage based on field observations have found their place in the literature. These studies are generally case studies carried out for all building types or a specific type in a certain region. Işık [24] evaluated the damage caused to adobe buildings in the earthquake zone. Zengin and Aydın [25] and Vuran et al. [26] investigated the effect of the quality of RC structures on structural damage in the earthquake region. Karaşin [27] evaluated the damage in RC structures in the province of Diyarbakır. Avcil et al. [28] examined the damage in different types of structures in the province of Kahramanmaraş. In their studies, Işık et al. [29,30] evaluated in detail the damage to the mosques and minarets in the province of Adıyaman, as well as that to the masonry structures in the province. Ince [31] examined the damage in reinforced concrete structures in the province of Adıyaman. Ivanov and Chow [32] evaluated the causes of damage in RC structures in the province of Adıyaman within the scope of earthquake civil engineering. Although there are no structural analyses in most of these studies, structural damage was investigated as a result of field investigations. In this paper, numerical analyses of the sample RC structure were carried out. Therefore, the aim is to reveal whether the target displacements caused by earthquakes in the structure are adequately represented.

Within the scope of this study, the causes of damage in RC structures were investigated in detail as a result of studies carried out by the authors in the field. Because the earthquakes affected a very large region, only the RC structures in the city center, Gölbaşı, and Kahta districts of Adıyaman were taken into account in this study. The structures were subjected to detailed observational examination. Considering all the parameters that will directly affect the behavior of the buildings under the influence of earthquakes, the cause-and-effect relationships of the structural damage have been revealed. In this context, the main causes of structural damage were evaluated under 11 different subheadings. Structural damage for each parameter was exemplified. The study also gave information about the earthquakes on 6 February 2023. In the study, numerical modeling was carried out for a sample RC building, using the measured and predicted PGA values. An attempt has been made to reveal at what levels the target displacements are sufficient or not. In this study, peak ground acceleration (PGA) and design spectral acceleration coefficients (S_{DS}) for Adıyaman districts were compared specifically for the last two earthquake hazards map that used in Türkiye.

2. 6 February 2023 Kahramanmaraş Earthquake and Its Effects on Adıyaman (Analysis of the Response Spectra and Strong Ground Motion Records)

The city of Adıyaman in the Central Euphrates region of south-eastern Anatolia is located between 37°25′–38°10′ N parallel and 37°27′–39°15′ E meridians. It is bordered by the Taurus Mountains in the north and the Euphrates in the east. The city has hosted many civilizations in the transition zone between the historical Anatolian geography and Mesopotamia. Mount Nemrut National Park, a world heritage site, is located within the borders of Adıyaman. The city's center has formed its development around Adıyaman Castle, an archaeological site today. Adıyaman city center, Gölbaşı, and Kahta districts constitute the scope of this study.

Adıyaman is located in the East Anatolian Fault Zone (EAFZ), one of Türkiye's two important fault zones. Specifically, Gölbaşı was built on one of the important segments of the EAFZ. The seismically active East Anatolian Fault Zone (EAFZ) is one of the most important active tectonic structures of the eastern Mediterranean region. The EAFZ, a left-lateral strike–slip fault, and the NAFZ, a right-lateral strike–slip fault, cause the Anatolian microplate to move westward. The EAFZ was first described as a transform fault by Arpat and Şaroğlu [33]. The 295 km long eastern section of the EAFZ, between Karlıova and Çelikhan, has a narrow deformation zone, observed as a single fault trace, except for the step-over structures (Figure 2). On the other hand, it divides into northern and southern fault strands in the west of Çelikhan and is observed as a 65 km wide deformation belt [34]. The southern strand, which is the main fault zone, has a total length of 580 km between Karlıova and Antakya and is divided into 7 fault segments called Karlıova, Ilıca, Palu, Pütürge, Erkenek, Pazarcık, and Amanos from N–E to S–W [34–36]. Segment lengths vary between 31 and 112 km, and their strikes vary between N–35° E and N–75° E. The northern strand, which is called the Sürgü-Misis Fault System, exhibits a left-lateral strike–slip fault segment of approximately 380 km between Çelikhan and İskenderun Bay [34]. The northern strand from N–E to S–W consists of 9 segments named Sürgü, Çardak, Göksun, Savrun, Çokak, Misis, Toprakkale, Yumurtalık, Karataş, and Düziçi-İskenderun fault segments [34–36]. While the northern strand of the EAFZ connects to the Misis-Girne zone via Iskenderun Bay, the southern strand joins with the Ölüdeniz fault zone in the Karasu tectonic depression area.

The shake map of the Kahramanmaraş earthquakes is shown in Figure 3 and the earthquakes that occurred in the earthquake region are shown in Figure 4.

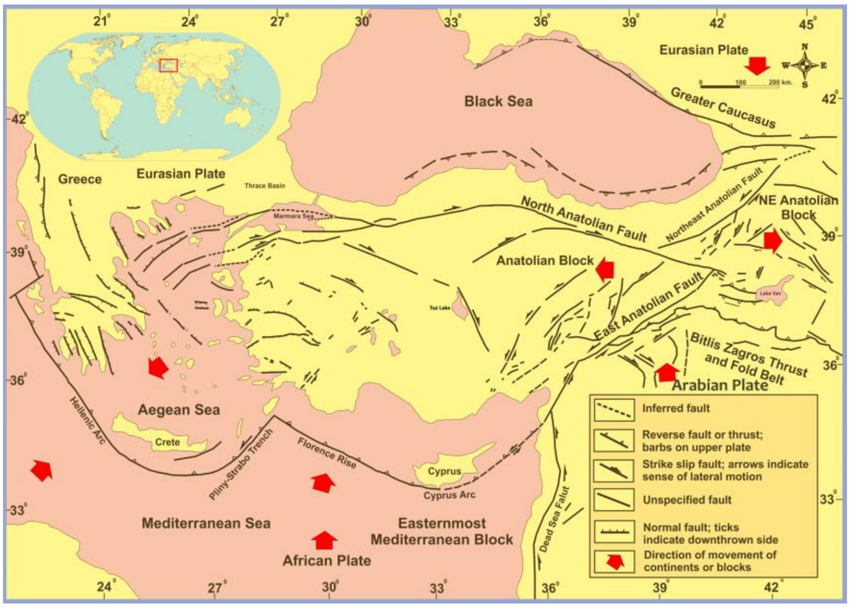

Figure 2. The tectonic system in which the Anatolian Block is located [37].

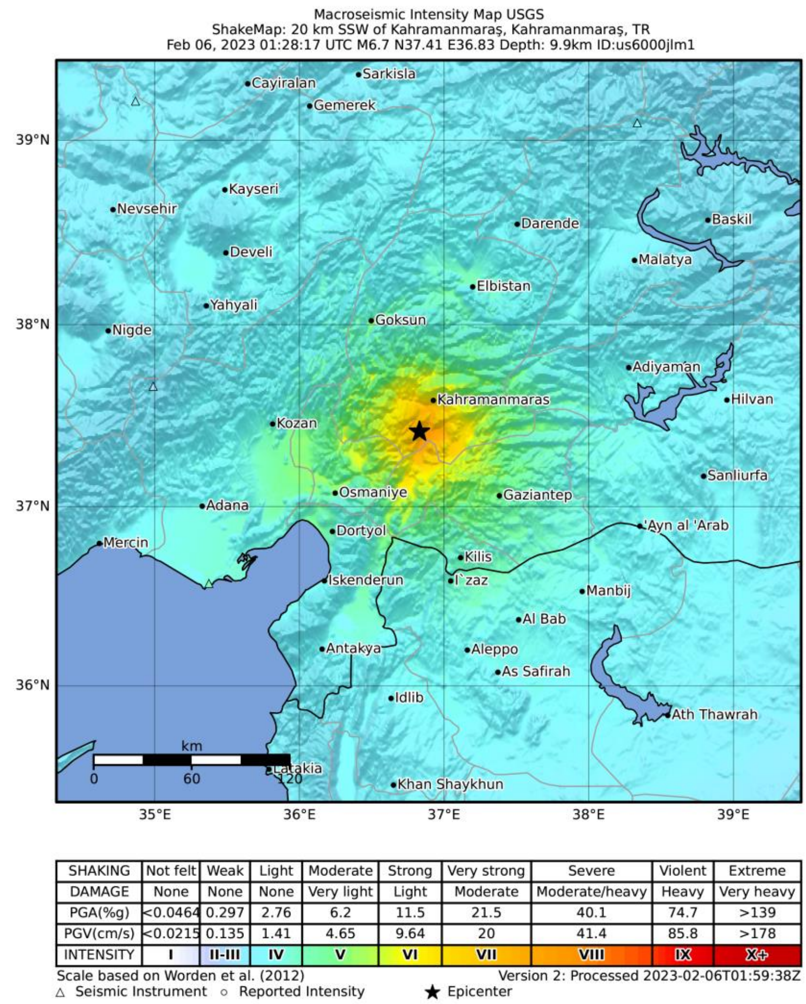

Figure 3. Shake map of the Kahramanmaraş earthquake [38].

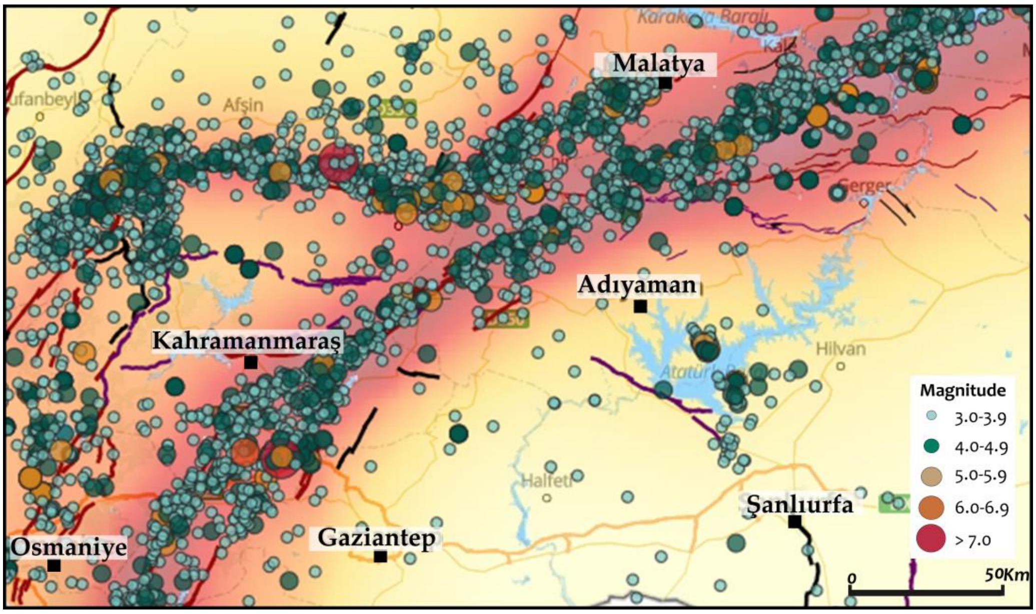

Figure 4. The East Anatolian Fault Zone and the epicentral distribution of the earthquakes that occurred [39].

After two main shocks with magnitudes of M_w = 7.7 and M_w = 7.6, acceleration according to accelerometers in the province of Adıyaman is shown in Table 1. In this paper, four different distance metrics have been considered: Joyner–Boore distance (R_{jb}), rupture distance (R_{rup}), epicentral distance (R_{epi}), and hypocentral distance (R_{hyp}).

Table 1. Measurement of earthquakes in city of Adıyaman.

District	Station Code	Longitude	Latitude	PGA (cm/s^2)			R (km)			
				NS	EW	UD	R_{jb}	R_{rup}	R_{epi}	R_{hyp}
06.02.2023 04:17 M_w = 7.7 (Pazarcık-Kahramanmaraş)										
Besni	2713	37.49254	37.62405	0.03	2.98	0.03	125.96	125.96	56.15	56.80
Gölbaşı	0208	37.78694	37.65275	30.20	14.00	16.97	147.38	147.38	77.26	77.73
Tut	0213	37.79667	37.92957	242.28	171.69	291.29	166.84	166.84	96.48	96.87
Centre	0201	37.76121	38.26742	474.12	879.95	318.97	189.97	189.97	120.12	120.42
Centre	0210	37.76720	38.28660	65.91	61.37	42.13	191.77	191.77	121.92	122.23
Çelikhan	0214	38.028298	38.22594	61.68	54.38	69.91	203.09	203.09	132.74	133.02
Sincik	0215	38.029958	38.55626	61.40	108.13	28.82	226.99	226.99	156.69	156.92
Sincik	0216	38.030907	38.557087	20.44	38.58	22.58	227.11	227.11	156.80	157.04
Sincik	0217	38.029958	38.556268	13.05	17.90	17.47	226.99	226.99	156.69	156.92
06.02.2023 13:24 M_w = 7.6 (Elbistan-Kahramanmaraş)										
Tut	0213	37.79667	37.92957	121.30	126.62	71.35	66.97	66.97	68.73	69.08
Samsat	0209	37.57763	38.48251	33.42	35.54	15.61	162.75	162.75	123.12	123.32
Kahta	0205	37.79177	38.61597	44.88	54.66	32.94	124.36	124.36	125.19	125.39

The peak ground acceleration (PGA) due to both earthquakes was measured as 879.95 cm/s^2 in the E-W direction of Adıyaman city center in the first earthquake. The second earthquake was measured as 126.62 cm/s^2 in the E-W direction in the Tut district of Adıyaman.

The PGA and peak ground velocities (PGVs) attained according to different probabilities of exceeding 50 years in the currently used Türkiye Earthquake Hazard Map for all districts in Adıyaman are given in Table 2. DD-1 is used for the earthquake ground motion level with a 2% probability of exceeding 50 years, and DD-2, DD-3, and DD-4 are the probabilities of exceedance of 10%, 50%, and 68%, respectively.

Table 2. The predicted PGA and PGV values for the districts of Adıyaman.

No	District	PGA (g)				PGV (cm/s)			
		2%	10%	50%	68%	2%	10%	50%	68%
1	Center	0.423	0.244	0.099	0.066	29.345	16.264	6.227	4.056
2	Besni	0.563	0.325	0.123	0.082	37.663	20.777	7.470	4.885
3	Çelikhan	1.062	0.592	0.209	0.126	77.713	41.893	11.332	6.395
4	Gerger	0.689	0.374	0.150	0.106	41.913	21.921	8.164	5.556
5	Gölbaşı	0.955	0.510	0.170	0.111	63.998	32.766	9.768	6.073
6	Kahta	0.423	0.241	0.098	0.067	27.644	15.435	6.028	4.023
7	Samsat	0.330	0.179	0.070	0.047	21.533	11.947	4.770	3.204
8	Sincik	1.101	0.612	0.210	0.131	71.420	38.623	11.149	6.400
9	Tut	0.910	0.492	0.159	0.101	58.434	30.665	9.223	5.594

According to the current earthquake hazard map, the PGA value for the standard design ground motion level (DD-2) is in the range of 0.17–0.61 g. The highest PGA values were obtained for Sincik, while the lowest values were obtained for Samsat.

Figure 5 shows the E–W, N–S, and vertical acceleration (u) spectra of the 6th February 2023 Pazarcık, Kahramanmaraş earthquake recorded at station 0201 in Adıyaman, their representations according to the different probabilities of exceedance, and acceleration graphs. According to the acceleration values, the highest acceleration for the E–W direction is 1.15 g, for the north–south direction 1.16 g, and for the vertical direction 0.66 g. Horizontal accelerations of the 0201 station exceeded the design spectra of DD-1, DD-2, and DD-3, while vertical accelerations exceeded the design spectra of DD-2 and DD-3.

The E–W, N–S, and vertical acceleration spectra of the 6 February 2023 Pazarcık, Kahramanmaraş earthquake recorded at the station 0208 of Gölbaşı, Adıyaman, their representations according to the different probability of exceedance, and acceleration graphs are shown in Figure 6. The acceleration values were measured as 0.04 g for the E–W direction, 0.11 g for the N–S direction, and 0.05 g for the vertical direction. It is seen that the acceleration values obtained do not exceed any design spectra values. However, Gölbaşı is located on extremely soft, shallow groundwater and liquefiable soils. V_s30 speed values are in the range of 180–360 m/s and are in ZD and sometimes ZE soil classes. In addition, due to the liquefaction potential, ZF soil classes are also quite dense. The acceleration station, where the acceleration is recorded, shows the ZC soil class feature. On the other hand, the average values of the soil conditions of 30 m show very low values near the surface and are likely to fall below the 180 m/s vs. velocity value. Therefore, regions of weak soil conditions, such as Gölbaşı district, where structures built with shallow foundations are located, cannot be expected to be represented by the acceleration value recorded in the acceleration station that is not in the same soil conditions. As is known, acceleration values are affected by ground conditions. Unless it is for special purposes, acceleration recorders are placed on relatively firmer ground. For this reason, it is obvious that the acceleration values recorded in Gölbaşı are inconsistent with the resulting damage distribution.

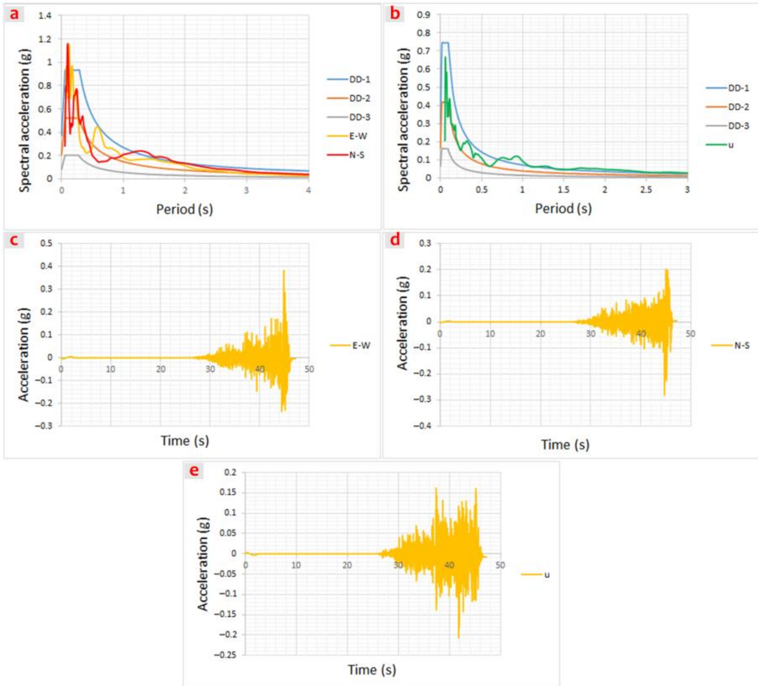

Figure 5. The comparison of earthquake spectral acceleration with design spectra. (**a**) Horizontal, (**b**) vertical of Adıyaman Downtown, the components of ground accelerations recorded at Adıyaman 0201 station, (**c**) E–W, (**d**) N–S, (**e**) Vertical directions.

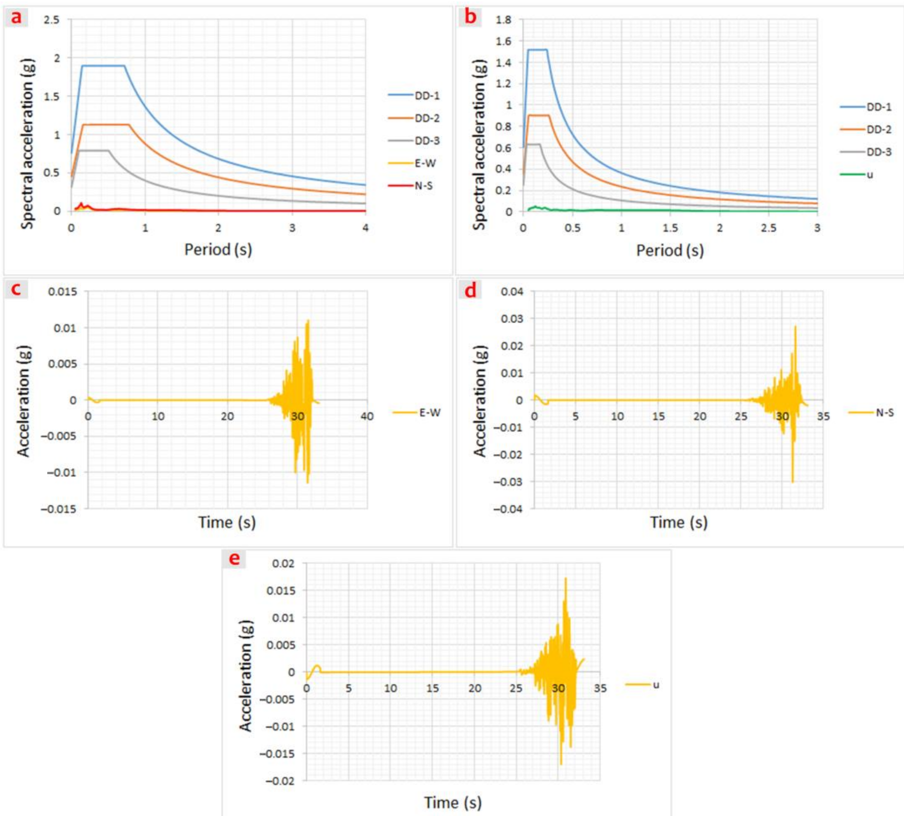

Figure 6. The comparison of earthquake spectral acceleration with design spectra. (**a**) Horizontal, (**b**) vertical of Gölbaşı, Adıyaman, the components of ground accelerations recorded at Gölbaşı 0208 station, (**c**) E–W, (**d**) N–S, (**e**) Vertical directions.

The E–W, N–S, and vertical acceleration spectra of the earthquake recorded at station 0205 of Kahta, Adıyaman, their representations according to the various probabilities of exceedance, and the acceleration graphs are shown in Figure 7. According to the acceleration values, the highest acceleration for E–W and N–S directions is 0.17 g and 0.11 g for the vertical direction. It is understood that the acceleration values obtained from this station do not exceed any of the design spectra values.

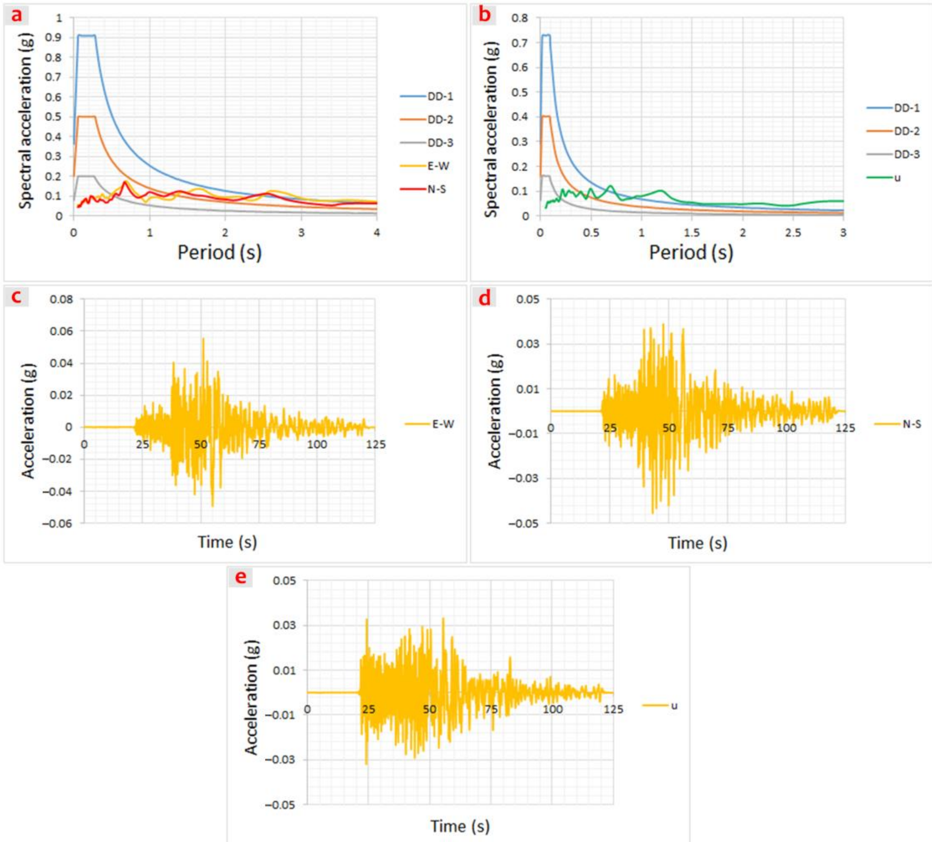

Figure 7. The comparison of earthquake spectral acceleration with design spectra. (**a**) Horizontal, (**b**) vertical of Kahta, Adıyaman, the components of ground accelerations recorded at Kahta 0205 station, (**c**) E–W, (**d**) N–S, (**e**) Vertical directions.

Considering the last two earthquake hazard maps used in Türkiye, the changes in the PGA and the design spectral acceleration coefficient (S_{DS}) for the short period (0.2 s) for the central locations of the settlements where the fieldwork was performed are shown in Table 3. For the comparison of the short-period values, the local soil class ZC, which is given in the Turkish Building Earthquake Code and can be considered the average soil class, has been taken into account.

In contrast to the present earthquake hazard map, the PGA and S_{DS} values indicated on the previous earthquake map increased for Gölbaşı, Besni, Çelikhan, Sincik, and Tut, while they reduced for Adıyaman/center, Gerger, Kahta, and Samsat districts. One of the most significant tectonic features in the nation, the East Anatolian Fault Zone, lies across much of the city of Adıyaman. The city of Adıyaman is situated along the Gölbaşı–Tür koğlu (90 km), Çelikhan–Erkenek (45 km), and Palu–Sincik (145 km) segments of the EAFZ. During the instrumental period, no earthquake damage was recorded (Adıyaman Provincial Level Disaster Risk Reduction Plan), with the exception of the 2004 Mw = 5.1 Çelikhan earthquake.

Table 3. Comparison of PGA and S_{DS} values based on the last two earthquake hazard maps.

No	District	TSDC-2007 Seismic Zone	TSDC-2007 PGA (g)	TBEC-2018 PGA (g)	PGA 2018/2007	S_{DS} 2007	S_{DS} 2018	S_{DS} 2018/2007
1	Center	2	0.300	0.244	0.81	0.75	0.734	0.98
2	Besni	2	0.300	0.325	1.08	0.75	0.925	1.23
3	Çelikhan	1	0.400	0.592	1.48	1.00	1.702	1.70
4	Gerger	1	0.400	0.374	0.94	1.00	1.069	1.10
5	Gölbaşı	1	0.400	0.510	1.10	1.00	1.462	1.50
6	Kahta	2	0.300	0.241	0.80	0.75	0.719	0.96
7	Samsat	2	0.300	0.179	0.60	0.75	0.534	0.71
8	Sincik	1	0.400	0.612	1.53	1.00	1.770	1.77
9	Tut	1	0.400	0.492	1.23	1.00	1.399	1.40

RC structures are commonly preferred in settlements with a city center of approximately 632.000. This earthquake caused great destruction for Adıyaman since the building stock in the rural areas did not receive engineering service and most of them were old and simple structures [40–42]. Over time, the buildings that completed their service life and were demolished in rural areas were replaced by mixed and reinforced concrete structures. Reinforced concrete structures constitute approximately 58% of the total building stock of Adıyaman cities and districts. Buildings are considered as collapsed, to be demolished, heavily damaged, moderately damaged, slightly damaged, undamaged, and having no detectable damage. This study is based on the data before 2 April 2023. No detectable damage refers to buildings whose damage cannot be determined due to different reasons. Building distributions according to damage levels are shown in Figure 8. Approximately 13% of the RC building stock in Adıyaman city center and its districts has become unusable. This shows the scale of the destruction in Adıyaman. About 74% of the RC building stock survived the earthquakes with slight or no damage.

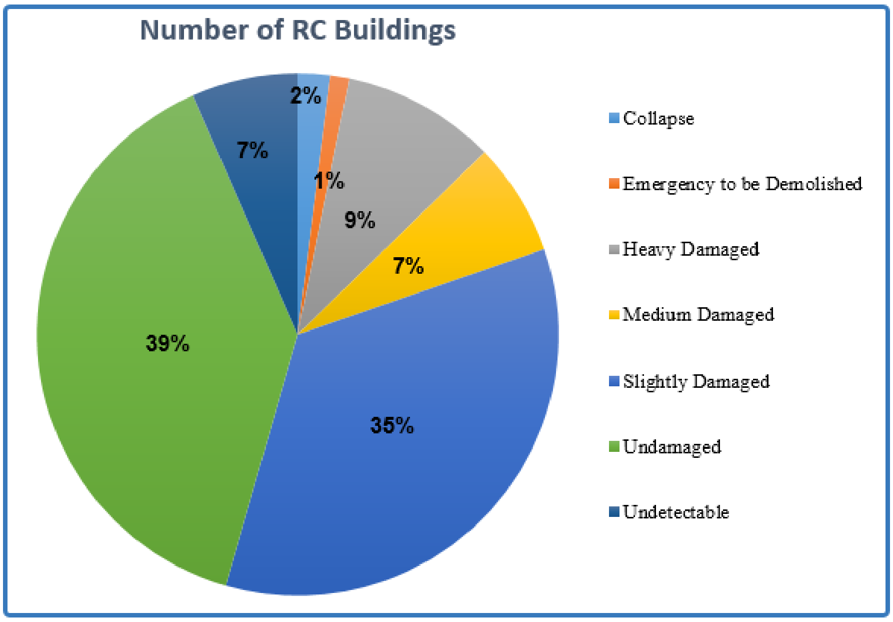

Figure 8. Damage distribution of reinforced concrete buildings in Adıyaman (by Adıyaman Provincial Directorate of Environment, Urbanization and Climate Change, 2023).

3. Damage in Reinforced Concrete Structures

Damage to RC structures is often divided into two categories: brittle failure of RC frame members and out-of-plane collapse of non-structural walls. The majority of RC building collapses that occur during earthquakes can be linked to poor-quality construction and the use of non-ductile detailing. The design and construction of RC moment-frame systems used little to no seismic design, according to an examination of collapsed and damaged buildings.

Different parameters were taken into account while examining the damage to the reinforced concrete structures in Adıyaman. Detailed explanations are given for each parameter and the cause–effect relationship of the damage was investigated.

3.1. Strength of the Concrete

The strength of the materials that make up the structures directly affects the seismic behavior of the structure. The weak point of reinforced concrete structures is the concrete material formed by many stages [43–46]. Coarse aggregate in larger sizes than necessary, which does not have an appropriate particle size distribution, has insufficient adherence between concrete and reinforcement (Figure 9).

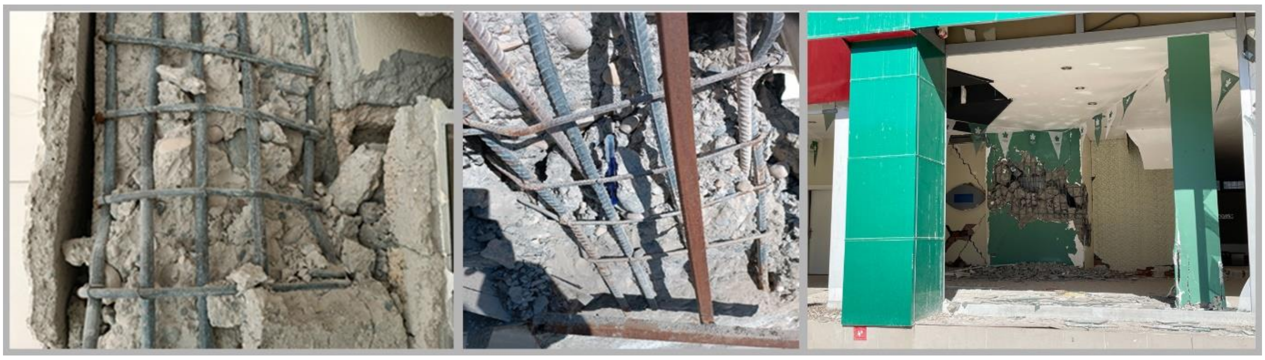

Figure 9. Inappropriate particle size distribution.

In concrete casting, failure to pay attention to significant issues such as preparation, transportation, temperature, weather conditions, casting time, compaction, taking test samples, post-casting maintenance, and curing also causes low concrete strength. As a result, the concrete did not provide sufficient strength due to segregation and buildings were built using poor-quality concrete with insufficient strength (Figure 10).

Figure 10. Examples of the use of poor-quality concrete and damage.

3.2. Reinforcement Problems

Reinforcements are used to resist tensile stresses in reinforced concrete. Inadequate and inappropriate reinforcement, as well as poor workmanship, increase reinforcement-related structural damage [47,48]. The buckling of the longitudinal rebars has been observed in the structural system elements, where sufficient stirrup reinforcement is not used. This damage, which occurs in the lower and upper parts of the column, where the earthquake-induced internal forces are greatest, is shown in Figure 11. In addition, the plain reinforcement rebar used in the reinforced concrete is one of the important reasons for the damage caused by the reinforcement and the low adherence between the concrete and the reinforcement. Particularly, it was observed that the outer column longitudinal steel bar buckled within the foundation height where stirrups were either missing or widely spaced.

Figure 11. Examples of damage caused by reinforcement.

3.3. Short Column Damage

Column dimensions may vary within a building due to a mezzanine floor, band-type window, or hill slope effect in buildings. Band-type windows made for lighting purposes, especially on the ground and basement floors, create different heights in the column, resulting in a short column mechanism [49–51]. Short column damage is shown in Figure 12. Despite the use of adequate reinforcement, the low concrete strength triggered this damage. Such captive column failures led to story collapses in some structures.

Figure 12. Examples of short column damage.

3.4. Soft/Weak Story

As a result of the stiffness and strength differences between the stories in buildings, significant differences occur between the relative story drifts. In this case, the soft story mechanism is formed and the ground floors in particular experience the collapse mechanism. This situation has been observed frequently in buildings where there are large commercial enterprises on the ground floors and there are residential sections on the upper floors [52–55]. In Adıyaman, it is observed that considerable structural damage occurred, notably in some RC buildings with high residual drift as a consequence of soft/weak stories. Such structural damage is shown in Figure 13.

Figure 13. Complete collapse of the ground story as a result of soft story damage.

3.5. Heavy Overhang

One of the causes of damage in reinforced-concrete-type structures is heavy overhangs in the structure. Heavy overhanging structures are generally seen in buildings where the upper-floor building areas are larger than the ground-floor building areas [56–58]. Damage occurring at different levels in these parts is shown in Figure 14.

Figure 14. Structural damage in RC structures due to heavy overhangs.

3.6. Pounding Effect

Adjacent structures collide with each other as a result of the pounding effect during an earthquake. The main problem here is that the floor levels in adjacent buildings are not the same. The shear forces that occur in structures with different floor levels create additional shear forces on the vertical structural members in the other structure, causing the shear capacity of these columns to be exceeded. It is observed that the damage occurred at dilatation joints where pounding had occurred between adjacent structures and the location of poor concrete consolidation during construction. Damage caused by the pounding effect is shown in Figure 15.

Figure 15. Examples of damage caused by the pounding effect.

3.7. Ground Failures

Low soil bearing capacity and insufficient foundation depth caused structural damage under lateral loads. Soil-related damages are shown in Figure 16. One of the reason of the damages is insufficient foundation depth prevented the structure from transferring the superstructure loads to the ground correctly. At the same time, although there is no structural damage to the structural system members, the structure is separated from its equilibrium position because the overturning moment capacity is exceeded as a result of both insufficient foundation depth and low soil bearing capacity. Soil-related damage is more common in Gölbaşı district. Some more soil-related damages observed in Gölbaşı after both major earthquakes is shown in Figure 16.

Figure 16. Examples of soil-related damage.

3.8. Failure of Reinforced Concrete Frame

Insufficient connections between the horizontal and vertical structural members of the reinforced concrete (RC) structural system mean that the frame members transfer loads independently. In this case, frame members that do not work together increase the probability of structural damage, causing the structure to suffer much more damage (Figure 17).

Figure 17. Failure due to insufficient RC frame.

3.9. Strong Beam–Weak Column Failure

Column–beam dimensions of RC frame systems must be compatible. This situation is explained in the regulations as the end moments required to carry the columns should be 20% more than the total beam end moments, and it is stated that the columns should be built stronger than the beams [59,60]. However, due to this situation, which was not taken into account during the project and implementation phase, heavy structural damage occurred as shown in Figure 18. As a result of this situation and frame failure, the floors collapsed on top of each other, causing pancake-style collapse.

Figure 18. Examples of strong beam–weak column failure.

3.10. Damage Due to Inadequate Concrete Cover and Adherence

The concrete cover is an important detail that protects the reinforcement from external effects and should be built as a part of the reinforced concrete. However, too little concrete cover, due to poor workmanship, is then covered with plaster [61]. As a result of this, with elements that cannot provide sufficient adherence between concrete and reinforcement, the concrete cover spills, and the structural element is damaged. Examples of such damage are shown in Figure 19.

Figure 19. Examples of damage caused by insufficient concrete cover.

In addition, insufficient concrete cover causes a loss of mass due to corrosion of the reinforcement over time, and as a result, it causes ruptures in the reinforcement and damage by separating it from the concrete. Such damage is shown in Figure 20.

Figure 20. Damage due to corroded reinforcement.

3.11. The Infill Wall Damage

The damage that occurs on the infill walls, which are used for the purpose of dividing and closing the spaces in reinforced concrete structures and which are considered only as a load in the building design, is shown in Figure 21. Infill walls, which are generally constructed of materials with low tensile and shear strength, increase the extent of damage to these members due to poor workmanship. The infill wall damage was widespread, including in- and out-of-plane failures.

Figure 21. Examples of infill wall damage in RC structures.

3.12. Buildings Providing Life Safety

Despite minor structural damage, the safety of life and property was preserved in the structures that were constructed in accordance with the technique requirements during the construction phase by receiving engineering services. In particular, the shear walls used in RC structures have positively supported the behavior of the structures under the influence of earthquakes. Example structures that provide life and property safety are shown in Figure 22.

Figure 22. RC buildings that provide life and property safety despite minor damage.

3.13. Secondary Effects of Earthquake

RC buildings that were heavily damaged and collapsed as a result of the earthquake also caused economic losses. In particular, many vehicles have become unusable due to damage by building debris. This damage is shown in Figure 23.

Figure 23. Examples of vehicles damaged by collapsed structures.

In light of all these evaluations, the main causes of damage to reinforced concrete structures are shown in Figure 24.

CAUSES OF DAMAGE		
Low strength concrete	Inadequate RC frame connection	Reinforcement problems
Short column damages	Lack of cross ties	Insufficient transverse reinforcement
Soft/weak story	Heavy overhang	Lack of transverse reinforcement
Pounding	Poor soil properties	Poor workmanship and low strength infill material
Strong beam - weak column	Insufficient docking RC frame	Use of flat reinforcement
Corrosion	90° hooks instead of 135°	Inadequate Concrete cover and adherence

Figure 24. Main causes of structural damage in RC buildings during Kahramanmaraş earthquakes.

4. Sample RC Structure Model

The purpose of earthquake-resistant building codes is to ensure that structures are built to withstand expected ground motion levels without experiencing damage. For the numerical analysis, SeismoStruct-2023 software was employed [62]. Using the acquired data, pushover analyses were performed on a 5-story sample RC building model. Every building under analysis had an identical story plan, which is shown in Figure 25. All slabs were selected as rigid diaphragms and the height of the slabs was selected as 120 mm.

All building models consider the story height to be 3 m. Five meters of span in each direction were taken into consideration when selecting the example reinforced concrete building, which was carried out symmetrically in the X and Y directions. Figure 26 displays the applied loads and the 2D and 3D building models for the 5-story building.

All structural designs were created using the infrmFBPH (force-based plastic hinge frame elements) for columns and beams. These components only allow for a finite amount of plasticity and simulate the spread inelasticity based on force. To represent the stress–strain distribution in the cross-section, the number of fibers in the cross-section should be sufficient [63]. For the parts that were chosen, a total of 100 fiber members are specified. This amount is adequate for these sections. The chosen plastic hinge length (Lp/L) was 16.67%. A totally fixed column footing and a free top end were the outcomes of setting the column's boundary conditions in line with the cantilever boundary criteria.

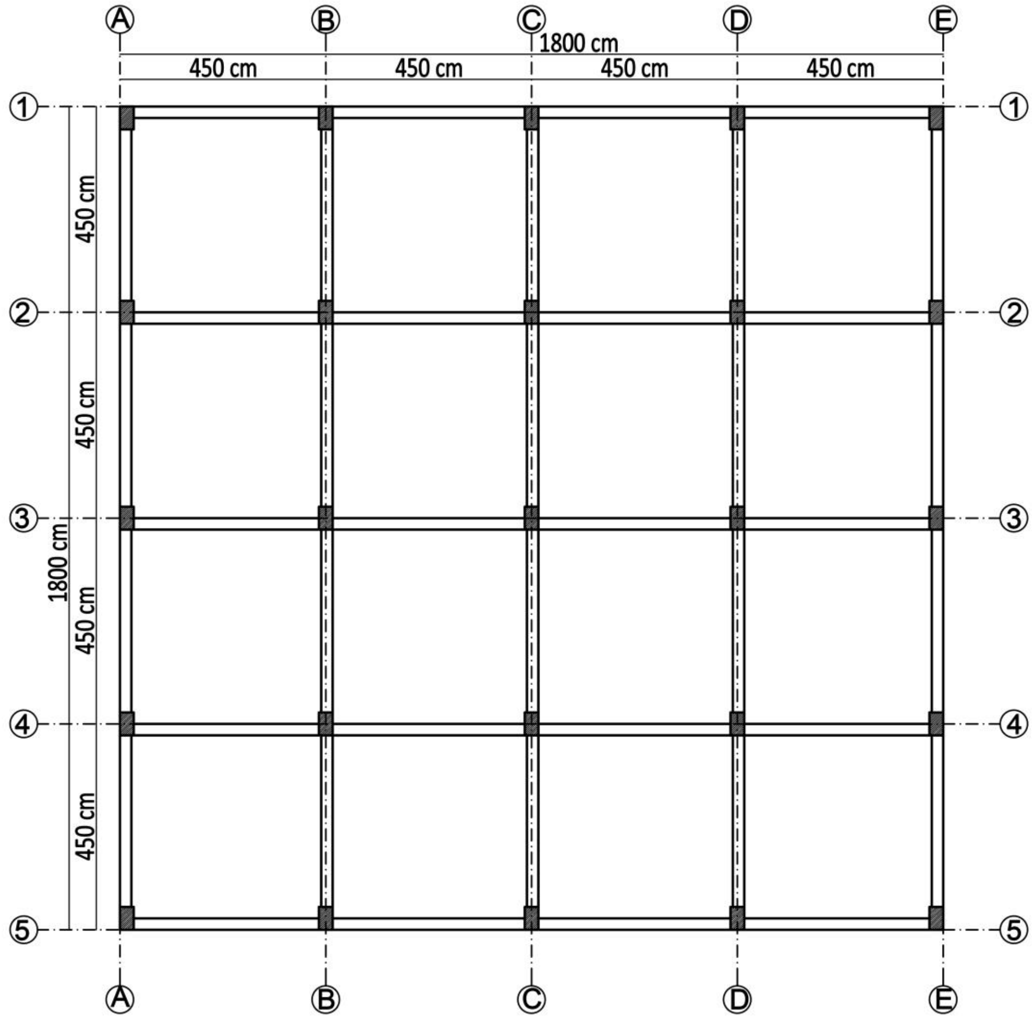

Figure 25. The blueprint of the sample RC building.

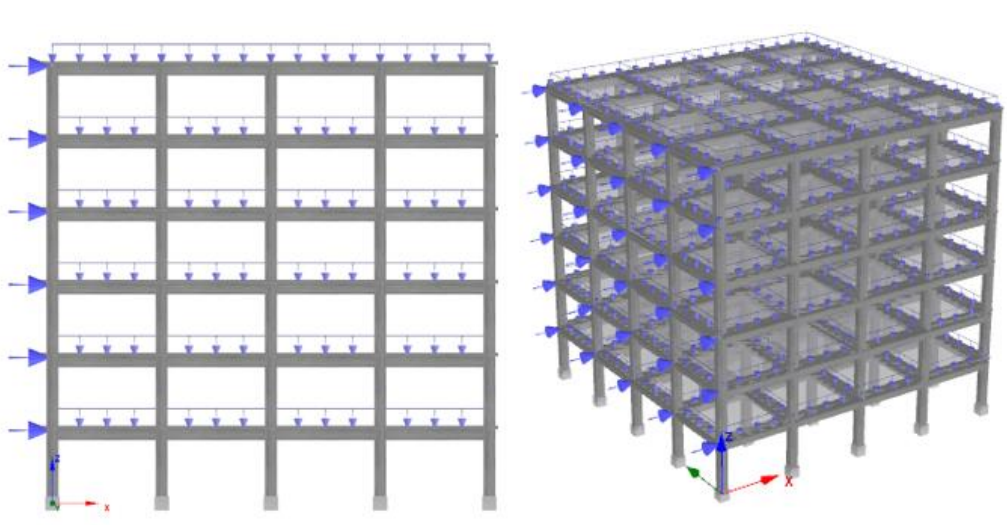

Figure 26. The 2D and 3D models of the sample RC building.

The characteristics of the reinforced concrete structure model are shown in Table 4.

Table 4. Analyzing the structural models' input data.

Parameters		Value
Concrete grade		C20/25
Reinforcement grade		S420
Beams		250 × 500 mm
Height of floor		120 mm
Cover thickness		25 mm
Columns		400 × 500 mm
Longitudinal reinforcement	Corners	4Φ20
	Top bottom side	4Φ16
	Left right side	4Φ16
Transverse reinforcement		Φ10/100
Material model (steel)		Menegotto-Pinto [64]
Material model (Concrete)		Mander et al. non-linear [65]
Constraint type		Rigid diaphragm
Local soil class		ZC
Incremental loads		5.0 kN
Permanent loads		5.0 kN/m
Target displacement (5-story)		0.30 m
Importance class		II
Damping		5%

Pushover analysis was used in all structural analyses. Pushover analysis captures the behavior of a structure from a fully elastic state to collapse. It is an approximate method of exposing the structure to lateral forces that increase step by step with a constant height distribution until the target displacement is reached. In addition to permanent loads due to gravity, incremental loads consisting of horizontal loads at each floor level are also applied to the structure in the X direction. Conventional (non-adaptive) pushover analysis is used to estimate the horizontal capacity of structures whose dynamic behavior is not significantly affected by the levels of deformations occurring (i.e., the shape of the horizontal load model that should simulate the dynamic behavior can be assumed to be constant) [66–68].

In performance-based earthquake engineering, it is crucial to predict the goal displacements for damage calculation when specific structural element performance limitations are met. In this investigation, the limit states provided in Eurocode 8 (Part 3) [69,70] were considered for damage estimation. Figure 27 displays the goal displacements, and Table 5 provides a description of these limit states.

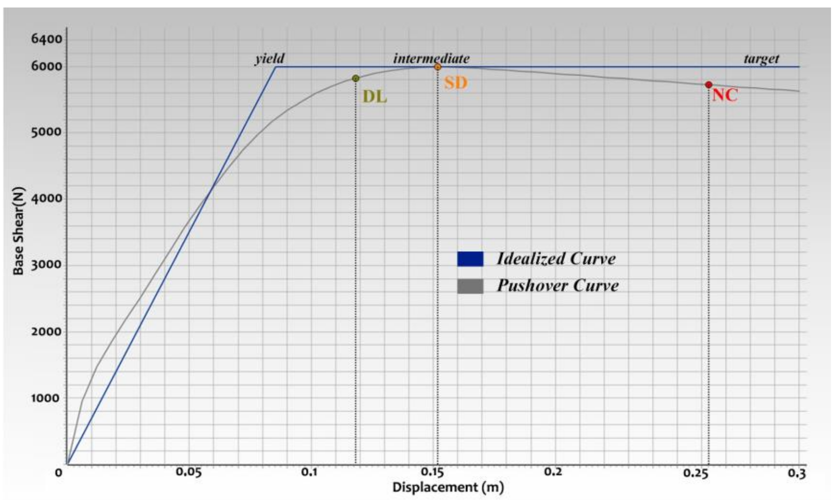

Figure 27. Target displacements on idealized and pushover curves.

Table 5. Suggested limit states in Eurocode 8 (Part 3) [69,70].

Limit State	Description	Return Period (Year)	Probability of Exceedance (in 50 Years)
Damage Limitation (DL)	Only lightly damaged, damage to non-structural components is economically repairable	225	0.20
Significant Damage (SD)	Significantly damaged, some residual strength and stiffness, non-structural components damaged, uneconomic to repair	475	0.10
Near collapse (NC)	Heavily damaged, very low residual strength and stiffness, large permanent drift but still standing	2475	0.02

The target displacements were attained one by one according to the PGAs anticipated in the last two earthquake hazard maps, taking into account the standard ground motion level for the geographical locations selected from each district of the province of Adıyaman. In order to make comparisons, structural analyses were carried out by taking into account the highest PGA values measured in the earthquake stations in those districts during earthquakes. In districts where there is no PGA measurement, the values in the nearest district are taken into account. All limit states obtained from structural analyses are shown in Table 6.

Table 6. The obtained target displacements of the sample RC model.

District	TBEC-2007, Suggested			TBEC-2018, Suggested			Measured PGA-2023		
	DL (m)	SD (m)	NC (m)	DL (m)	SD (m)	NC (m)	DL (m)	SD (m)	NC (m)
Center	0.084	0.108	0.187	0.068	0.087	0.152	0.249	0.319	0.553
Besni	0.084	0.108	0.187	0.091	0.117	0.202	0.003	0.004	0.006
Çelikhan	0.112	0.143	0.249	0.165	0.212	0.368	0.020	0.025	0.044
Gerger	0.112	0.143	0.249	0.105	0.134	0.233	0.015	0.020	0.034
Gölbaşı	0.112	0.143	0.249	0.143	0.183	0.317	0.008	0.010	0.019
Kahta	0.084	0.108	0.187	0.067	0.086	0.150	0.015	0.020	0.034
Samsat	0.084	0.108	0.187	0.050	0.064	0.111	0.009	0.011	0.020
Sincik	0.112	0.143	0.249	0.171	0.219	0.380	0.031	0.039	0.068
Tut	0.112	0.143	0.249	0.137	0.176	0.306	0.036	0.047	0.081

The target displacement values obtained from the measured values in all districts except the Adıyaman central district are provided with the predicted values on both maps. As a result of the analysis for DD-1 for Adıyaman city center, target displacements were obtained as DL = 0.118 m, SD = 0.152 m, and NC = 0.263 m, respectively. The predicted values for the DD-1 ground motion level for Adıyaman city center did not meet the measured values.

5. Conclusions

Structures under the influence of earthquakes may show structural system weaknesses due to design, construction defects, and environmental effects. In addition, the negative structural factors caused by a change in the building function also cause damage in earthquakes. Unsuitable design, using low-strength materials, poor workmanship, and lack of inspection constitute the destructive roles of damage. The appropriate structural features of the structures exposed to a possible earthquake will reduce the loss of life and property.

In addition, obtaining the local soil conditions realistically will make the structural design and evaluation meaningful.

It has been observed that the reinforced concrete structures which were examined in the settlements where fieldwork was carried out for damage assessment were damaged, especially due to low concrete strength, insufficient reinforcement, and low earthquake resistance. Especially in core concrete, crushing and segregation show that the concrete strength is very low. In addition, the use of plain reinforcement and the low adherence between concrete and reinforcement are the main causes of damage.

One of the primary reasons for the high level of destruction in the city center housing was commercial structuring that led to the formation of soft floors. In order to avoid this situation in new settlements, commercial structures should be arranged independently from residences.

Columns in frame structures may be stretched up to their plastic moment capacity when subjected to horizontal loads. An immense moment gradient and hence a significant shear force occur in the case of short columns with significant bending capacity. Before the plastic moment capacity is achieved, a shear fracture frequently occurs. Therefore, it is best to avoid using short columns. The shear capacity must be enhanced to account for the excessive strength of the vertical reinforcement. An alternative is to design and detail the columns following capacity design criteria.

When necessary, dilatation joints appropriate for their technique should be used; otherwise, adjacent constructions should be abandoned. Additionally, it is important to make sure that the floors of all nearby structures are level with one another. Otherwise, it will be inevitable that the additional shear forces that will occur due to the pounding effect from the neighboring floors during the earthquake will cause significant damage.

The construction of heavy overhanging buildings, which are common in cities and districts, should be abandoned. The prohibition of making mezzanine floors and floor height changes within the building to prevent soft/weak floor formations in buildings other than commercial and industrial buildings will provide additional benefits in preventing loss of property and life after earthquakes.

It should be made mandatory for the masters who have the Vocational Qualification Certificate to take part in the building inspection system, and these masters should be responsible for the part that concerns them. In this way, it will be possible to carry out production following the project with a sense of responsibility.

In the current earthquake regulation, there is no obligation to use reinforced concrete shear walls. Attention should be paid to constructing reinforced concrete shears that will serve as earthquake shear walls at the rates to be determined in all kinds of reinforced concrete buildings to be built in the new design phase.

In concrete casting, adequate supervision should be carried out to pay maximum attention to vital issues such as preparation, transportation, temperature, weather conditions, casting time, compaction, taking test sampling, post-casting maintenance, and curing.

As plastic deformations frequently result in unpredictable behavior, additional displacements, and stress in the building structure, foundation structures must constantly stay elastic. Additionally, foundation repairs are far more challenging than building structural repairs. This calls for strengthening the reinforcement immediately beneath the plastic zones and detailing it suitably.

Sandy or silty soils that have been saturated with water may have a sufficient ability to carry a static load. However, they suddenly behave like a liquid when shaken, such as during an earthquake. If the soil is unevenly or inhomogeneously liquefied, buildings might tilt or completely collapse, which is frequently unavoidable. Therefore, the possibility of liquefaction of such soils should be investigated. Precautions should be taken against soil-related problems when necessary with measures such as injections, piled foundations, etc.

Target displacements are especially important in order to realistically reveal the seismic performance of structures under a possible earthquake. Target displacements were obtained by taking into account the last two earthquake hazard maps used in Türkiye and the

PGA values measured in the February 6 Kahramanmaraş earthquakes in the province of Adıyaman. It can be stated that the earthquake hazard is not adequately represented only in Adıyaman city center. The earthquake hazard taken into account in the design of buildings in all other districts of the province of Adıyaman has been taken into account at a sufficient level. This situation is also reflected in target displacements.

Some precautions should be taken regarding existing structures before a possible earthquake in the region. For example, with the health monitoring of the buildings, the changes after the use of the building can be followed. In this context, by making QR codes and similar applications, it will be possible to transfer this information to the system by checking the structures at specific intervals after they are used.

In conclusion, many buildings still stand in the region's seismically active areas built or planned according to past seismic laws. These structures should be appropriately fortified as soon as possible to prevent more casualties. Unquestionably, earthquake-resistant building design has increased in importance with the earthquakes in Türkiye on 6th February 2023.

Author Contributions: Conceptualization, E.I., H.B., A.B. and R.İ.; methodology, E.I., F.A., A.B. and E.A.; validation, A.B., R.İ. and E.H.; investigation, E.I., F.A., A.B. and E.A.; resources, H.B. and R.İ.; data curation, E.H. and E.A.; writing—original draft preparation, H.B., E.I., A.B. and F.A.; writing—review and editing, E.A. and R.İ.; visualization, E.A. and F.A.; supervision, E.I., A.B. and F.A.; funding acquisition, E.H. All authors have read and agreed to the published version of the manuscript.

Funding: This research received no external funding.

Institutional Review Board Statement: Not applicable.

Informed Consent Statement: Not applicable.

Data Availability Statement: The original contributions presented in the study are included in the article, further inquiries can be directed to the corresponding authors.

Acknowledgments: We would like to thank Adıyaman Provincial Director of Environment, Urbanization, and Climate Change, Faysal Ergezen, for his important contributions to the study.

Conflicts of Interest: The authors declare no conflicts of interest.

References

1. Bessason, B.; Bjarnason, J.Ö. Seismic vulnerability of low-rise residential buildings based on damage data from three earthquakes (Mw6.5, 6.5 and 6.3). *Eng. Struct.* **2016**, *111*, 64–79. [CrossRef]
2. Hadzima-Nyarko, M.; Mišetić, V.; Morić, D. Seismic vulnerability assessment of an old historical masonry building in Osijek, Croatia, using Damage Index. *J. Cult. Herit.* **2017**, *28*, 140–150. [CrossRef]
3. Binici, B.; Yakut, A.; Kadas, K.; Demirel, O.; Akpinar, U.; Canbolat, A.; Yurtseven, F.; Oztaskin, O.; Aktas, S.; Canbay, E. Performance of RC buildings after Kahramanmaraş Earthquakes: Lessons toward performance based design. *Earthq. Eng. Eng. Vib.* **2023**, *22*, 883–894. [CrossRef]
4. Ademović, N.; Kalman Šipoš, T.; Hadzima-Nyarko, M. Rapid assessment of earthquake risk for Bosnia and Herzegovina. *Bull. Earthq. Eng.* **2020**, *18*, 1835–1863. [CrossRef]
5. Cavallaro, A.; Fiamingo, A.; Grasso, S.; Massimino, M.R.; Sammito, M.S.V. Local site amplification maps for the volcanic area of Trecastagni, south-eastern Sicily (Italy). *Bull. Earthq. Eng.* **2024**, *22*, 1635–1676. [CrossRef]
6. Alih, S.C.; Vafaei, M. Performance of reinforced concrete buildings and wooden structures during the 2015 Mw 6.0 Sabah earthquake in Malaysia. *Eng. Fail. Anal.* **2019**, *102*, 351–368. [CrossRef]
7. Vlachakis, G.; Vlachaki, E.; Lourenço, P.B. Learning from failure: Damage and failure of masonry structures, after the 2017 Lesvos earthquake (Greece). *Eng. Fail. Anal.* **2020**, *117*, 104803. [CrossRef]
8. Jara, J.M.; Hernández, E.J.; Olmos, B.A.; Martínez, G. Building damages during the September 19, 2017 earthquake in Mexico City and seismic retrofitting of existing first soft-story buildings. *Eng. Struct.* **2020**, *209*, 109977. [CrossRef]
9. Yurdakul, Ö.; Duran, B.; Onur Tunaboyu, O.; Avşar, Ö. Field reconnaissance on seismic performance of RC buildings after the January 24, 2020 Elazığ-Sivrice earthquake. *Nat. Hazards* **2021**, *105*, 859–887. [CrossRef]
10. Liu, C.; Fang, D.; Zhao, L. Reflection on earthquake damage of buildings in 2015 Nepal earthquake and seismic measures for post-earthquake reconstruction. *Structures* **2021**, *30*, 647–658. [CrossRef]
11. Mertol, H.C.; Tunc, G.; Akis, T. Damage Observation of Reinforced Concrete Buildingsafter 2020 Sivrice (Elazığ) Earthquake, Türkiye. *J. Perform. Constr. Facil.* **2021**, *35*, 5. [CrossRef]

12. Bayrak, O.F.; Bikçe, M.; Erdem, M.M. Failures of structures during the January 24, 2020, Sivrice (Elazığ) Earthquake in Türkiye. *Nat. Hazards* **2021**, *108*, 1943–1969. [CrossRef]
13. Dogan, G.; Ecemis, A.S.; Korkmaz, S.Z.; Arslan, M.H.; Korkmaz, M.H. Buildings Damages after Elazığ, Türkiye Earthquake on January 24, 2020. *Nat. Hazards* **2021**, *109*, 161–200. [CrossRef]
14. Erkut Sayın, E.; Yön, B.; Onat, O.; Gör, M.; Öncü, M.E.; Tunç, E.T.; Bakır, D.; Karaton, M.; Calayır, Y. 24 January 2020 Sivrice-Elazığ, Türkiye earthquake: Geotechnical evaluation and performance of structures. *Bull. Earthq. Eng.* **2021**, *19*, 657–684. [CrossRef]
15. Caglar, N.; Vural, I.; Kirtel, O.; Saribiyik, A.; Sumer, Y. Structural damages observed in buildings after the January 24, 2020 Elazığ-Sivrice earthquake in Türkiye. *Case Stud. Constr. Mater.* **2023**, *18*, e018862023. [CrossRef]
16. Gurbuz, T.; Cengiz, A.; Kolemenoglu, Ş.; Demir, C.; Ilki, A. Damages and Failures of Structures in İzmir (Türkiye) during the October 30, 2020 Aegean Sea Earthquake. *J. Earthq. Eng.* **2023**, *27*, 1565–1606. [CrossRef]
17. Milani, G. Lesson learned after the Emilia-Romagna, Italy, 20–29 May 2012 earthquakes: A limit analysis insight on three masonry churches. *Eng. Fail. Anal.* **2013**, *34*, 761–778. [CrossRef]
18. Milani, G.; Valente, M. Failure analysis of seven masonry churches severely damaged during the 2012 Emilia-Romagna (Italy) earthquake: Non-linear dynamic analyses vs conventional static approaches. *Eng. Fail. Anal.* **2015**, *54*, 13–56. [CrossRef]
19. Monaco, P.; Totani, G.; Barla, G.B.; Cavallaro, A.; Costanzo, A.; Donofrio, A.; Evangelista, L.; Foti, S.; Grasso, S.; Lanzo, G.; et al. Geotechnical aspects of 2009 l'Aquila Earthquake. In *Special Topics in Earthquake Engineering, Geotechnical, Geological and Earthquake Engineering*; Springer: Berlin/Heidelberg, Germany, 2010; Volume 400.
20. Livaoğlu, R.; Timurağaoğlu, M.Ö.; Serhatoğlu, C.; Döven, M.S. Damage during the 6–24 February 2017 Ayvacık (Çanakkale) earthquake swarm. *Nat. Hazards Earth Syst. Sci.* **2018**, *18*, 921–934. [CrossRef]
21. Cavallaro, A.; Capilleri, P.P.; Grasso, S. Site characterization by dynamic in situ and laboratory tests for liquefaction potential evaluation during Emilia Romagna earthquake. *Geosciences* **2018**, *8*, 242. [CrossRef]
22. Piccinini, F.; Gorreja, A.; Di Stefano, F.; Pierdicca, R.; Sanchez Aparicio, L.J.; Malinverni, E.S. Preservation of Villages in Central Italy: Geomatic Techniques' Integration and GIS Strategies for the Post-Earthquake Assessment. *ISPRS Int. J. Geo-Inf.* **2022**, *11*, 291. [CrossRef]
23. Pan, Z.; Lang, Q.; Zhang, Y.; Zhang, J.; Yu, C.; Wu, C. Geological Hazard Assessment of Secondary Collapses Due to Volcanic Earthquakes on Changbai Mountain in China. *ISPRS Int. J. Geo-Inf.* **2023**, *12*, 307. [CrossRef]
24. Işık, E. Structural failures of adobe buildings during the February 2023 Kahramanmaraş (Türkiye) earthquakes. *Appl. Sci.* **2023**, *13*, 8937. [CrossRef]
25. Zengin, B.; Aydin, F. The effect of material quality on buildings moderately and heavily damaged by the Kahramanmaraş Earthquakes. *Appl. Sci.* **2023**, *13*, 10668. [CrossRef]
26. Vuran, E.; Serhatoğlu, C.; Timurağaoğlu, M.Ö.; Smyrou, E.; Bal, İ.E.; Livaoğlu, R. Damage observations of RC buildings from 2023 Kahramanmaraş earthquake sequence and discussion on the seismic code regulations. *Bull. Earthq. Eng.* **2024**, 1–30. [CrossRef]
27. Karasin, I.B. Comparative Analysis of the 2023 Pazarcık and Elbistan Earthquakes in Diyarbakır. *Buildings* **2023**, *13*, 2474. [CrossRef]
28. Avcil, F.; Işık, E.; İzol, R.; Büyüksaraç, A.; Arkan, E.; Arslan, M.H.; Aksoylu, C.; Eyisuren, O.; Harirchian, E. Effects of the February 6, 2023, Kahramanmaraş earthquake on structures in Kahramanmaraş city. *Nat. Hazards* **2024**, *120*, 2953–2991. [CrossRef]
29. Işık, E.; Avcil, F.; Arkan, E.; Büyüksaraç, A.; İzol, R.; Topalan, M. Structural Damage Evaluation of Mosques and Minarets in Adıyaman due to the 06 February 2023 Kahramanmaraş Earthquakes. *Eng. Fail. Anal.* **2023**, *151*, 107345. [CrossRef]
30. Işık, E.; Avcil, F.; Büyüksaraç, A.; İzol, R.; Arslan, M.H.; Aksoylu, C.; Harirchian, E.; Eyisuren, O.; Arkan, E.; Gngur, M.; et al. Structural damages in masonry buildings in Adıyaman during the Kahramanmaraş (Turkiye) earthquakes (Mw 7.7 and Mw 7.6) on 06 February 2023. *Eng. Fail. Anal.* **2023**, *151*, 107405. [CrossRef]
31. Ince, O. Structural damage assessment of reinforced concrete buildings in Adıyaman after Kahramanmaraş (Türkiye) Earthquakes on 6 February 2023. *Eng. Fail. Anal.* **2024**, *156*, 107799. [CrossRef]
32. Ivanov, M.L.; Chow, W.K. Structural damage observed in reinforced concrete buildings in Adiyaman during the 2023 Turkiye Kahramanmaras Earthquakes. In *Structures*; Elsevier: Amsterdam, The Netherlands, 2023; Volume 58, p. 105578.
33. Arpat, E.; Saroglu, F. The East Anatolian fault system: Thoughts on its development. *Bull. Miner. Res. Explor. Inst. Turk.* **1972**, *78*, 33–39.
34. Duman, T.Y.; Emre, Ö. *The East Anatolian Fault: Geometry, Segmentation and Jog Characteristics*; Geological Society, London, Special Publications: London, UK, 2013; Volume 372, pp. 495–529.
35. Emre, Ö.; Duman, T.Y.; Özalp, S.; Elmacı, H.; Olgun, Ş.; Şaroğlu, F. *Active Fault Map of Türkiye with Explanatory Text*; General Directorate of Mineral Research and Exploration Special Publication Series; General Directorate of Mineral Research and Exploration: Ankara, Turkey, 2013.
36. Emre, Ö.; Duman, T.Y.; Özalp, S.; Şaroğlu, F.; Olgun, Ş.; Elmacı, H.; Çan, T. Active fault database of Türkiye. *Bull. Earthq. Eng.* **2018**, *16*, 3229–3275. [CrossRef]
37. Akar, F.; Işık, E.; Avcil, F.; Büyüksaraç, A.; Arkan, E.; İzol, R. Geotechnical and structural damages caused by the 2023 Kahramanmaraş Earthquakes in Gölbaşı (Adıyaman). *Appl. Sci.* **2024**, *14*, 2165. [CrossRef]
38. Available online: https://earthquake.usgs.gov/earthquakes/eventpage/us6000jllz/executive (accessed on 30 April 2023).
39. Available online: https://www.afad.gov.tr/ (accessed on 30 April 2023).

40. Isik, E.; Buyuksarac, A.; Avcil, F.; Arkan, E.; Aydin, M.C.; Ulu, A.E. Damage evaluation of masonry buildings during Kahramanmaras (Turkiye) earthquakes on February 06, 2023. *Earthq. Struct.* **2023**, *25*, 209–221.
41. Türkiye Cumhuriyeti Cumhurbaşkanlığı. Available online: https://www.sbb.gov.tr/wp-content/uploads/2023/03/2023-Kahramanmaras-ve-Hatay-Depremleri-Raporu.pdf (accessed on 20 April 2023).
42. Peker, O.; Altan, M.F. The effect of errors in structural system design on the structure damaged in 2023 Turkey earthquakes: A case study. *Eng. Fail. Anal.* **2024**, *157*, 107923. [CrossRef]
43. Su, N. Structural evaluations of reinforced concrete buildings damaged by Chi-Chi earthquake in Taiwan. *Pract. Period. Struct.* **2001**, *6*, 119–128. [CrossRef]
44. Ates, S.; Kahya, V.; Yurdakul, M.; Adanur, S. Damages on reinforced concrete buildings due to consecutive earthquakes in Van. *Soil Dyn.* **2013**, *53*, 109–118. [CrossRef]
45. Varum, H.; Dumaru, R.; Furtado, A.; Barbosa, A.R.; Gautam, D.; Rodrigues, H. Seismic performance of buildings in Nepal after the Gorkha earthquake. In *Impacts and Insights of the Gorkha Earthquake*; Elsevier: Amsterdam, The Netherlands, 2018; pp. 47–63.
46. Çağatay, İ.H. Experimental evaluation of buildings damaged in recent earthquakes in Turkey. *Eng. Fail. Anal.* **2005**, *12*, 440–452. [CrossRef]
47. Çelebi, E.; Aktas, M.; Çağlar, N.; Özocak, A.; Kutanis, M.; Mert, N.; Özcan, Z. October 23, 2011 Türkiye/Van–Ercis earthquake: Structural damages in the residential buildings. *Nat. Hazards* **2013**, *65*, 2287–2310. [CrossRef]
48. Sezen, H.; Whittaker, A.S.; Elwood, K.J.; Mosalam, K.M. Performance of reinforced concrete buildings during the August 17, 1999 Kocaeli, Turkey earthquake, and seismic design and construction practise in Turkey. *Eng. Struct.* **2003**, *25*, 103–114. [CrossRef]
49. Ghobarah, A.; Galal, K.E. Seismic rehabilitation of short rectangular RC columns. *J. Earthq. Eng.* **2004**, *8*, 45–68. [CrossRef]
50. Chen, C.Y.; Liu, K.C.; Liu, Y.W.; Huang, W.J. A case study of reinforced concrete short column under earthquake using experimental and theoretical investigations. *Struct. Eng. Mech.* **2010**, *36*, 197–206. [CrossRef]
51. Işık, E.; Ulutaş, H.; Harirchian, E.; Avcil, F.; Aksoylu, C.; Arslan, M.H. Performance-based assessment of RC building with short columns due to the different design principles. *Buildings* **2023**, *13*, 750. [CrossRef]
52. Özmen, H.B.; Inel, M.; Demirtaş, Y. Evaluation of different cases of soft story formation for mid-rise RC buildings. *Res. Eng. Struct. Mater.* **2020**, *6*, 229–240.
53. Uzun, M.; Cogurcu, M.T. Investigation of effect of infilled wall on soft story irregularity. *J. Eng. Res. Appl. Sci.* **2018**, *7*, 878–885.
54. Tezcan, S.; Yazıcı, A.; Özdemir, Z.; Erkal, A. Zayıf kat- yumuşak kat düzensizliği. In Proceedings of the Altıncı Ulusal Deprem Mühendisliği Konferansı, İstanbul, Turkey, 17–22 October 2007; pp. 339–350.
55. Özmen, H.B.; İnel, M.; Bilgin, H. Yumuşak kat davranışının duvar etkisi dikkate alınarak incelenmesi. In Proceedings of the Altıncı Ulusal Deprem Mühendisliği Konferansı, İstanbul, Turkey, 17–22 October 2007; pp. 423–434.
56. Doğangün, A. Performance of reinforced concrete buildings during the May 1, 2003 Bingöl earthquake in Türkiye. *Eng. Struct.* **2004**, *26*, 841–856. [CrossRef]
57. Yakut, A.; Sucuoğlu, H.; Binici, B.; Canbay, E.; Donmez, C.; İlki, A.; Caner, A.; Celik, O.C.; Ay, B. Performance of structures in İzmir after the Samos island earthquake. *Bull. Earthq. Eng.* **2022**, *20*, 7793–7818. [CrossRef] [PubMed]
58. İnel, M.; Ozmen, H.B.; Bilgin, H. Re-evaluation of building damage during recent earthquakes in Türkiye. *Eng. Struct.* **2008**, *30*, 412–427. [CrossRef]
59. Zhang, C.; Tao, M.X. Strong-column–weak-beam criterion for reinforced concrete frames subjected to biaxial seismic excitation. *Eng. Struct.* **2021**, *241*, 112481. [CrossRef]
60. TBEC. *Turkish Building Earthquake Code*; T.C. Resmi Gazete: Ankara, Türkiye, 2018.
61. Işık, E.; Harirchian, E.; Bilgin, H.; Kaya, B.; Karaşin, İ.B. The effect of insufficient cover thickness on structural performance of reinforced concrete buildings. In Proceedings of the International Conference on Organization and Technology of Maintenance, Osijek, Croatia, 10 December 2021; Springer: Cham, Switzerland, 2022; pp. 262–277.
62. Seismosoft. SeismoStruct 2022—A Computer Program for Static and Dynamic Nonlinear Analysis of Framed Structures. 2022. Available online: http://www.seismosoft.com (accessed on 10 February 2024).
63. Antoniou, S.; Pinho, R. *Seismostruct–Seismic Analysis Program by Seismosoft*; Technical Manual and User Manual; Seismosoft: Pavia, Italy, 2022.
64. Menegotto, M.; Pinto, P.E. Method of analysis for cyclically loaded RC plane frames including changes in geometry and non-elastic behavior of elements under combined normal force and bending. In *Symposium on the Resistance and Ultimate Deformability of Structures Acted on by Well-defined Repeated Loads*; International Association for Bridge and Structural Engineering: Zurich, Switzerland, 1973; pp. 15–22.
65. Mander, J.B.; Priestley, M.J.N.; Park, R. Theoretical stress-strain model for confined concrete. *J. Struct. Eng.* **1998**, *114*, 1804–1825. [CrossRef]
66. Habibi, A.; Saffari, H.; Izadpanah, M. Optimal lateral load pattern for pushover analysis of building structures. *Steel Compos. Struct.* **2019**, *32*, 67–77.
67. Antoniou, S.; Pinho, R. Advantages and limitations of adaptive and non-adaptive force-based pushover procedures. *J. Earthq. Eng.* **2004**, *8*, 497–522. [CrossRef]
68. Papanikolaou, V.K.; Elnashai, A.S.; Pareja, J.F. Evaluation of conventional and adaptive pushover analysis II: Comparative results. *J. Earthq. Eng.* **2006**, *10*, 127–151. [CrossRef]

69. *EN 1998-3*; Eurocode-8: Design of Structures for Earthquake Resistanc—Part 3: Assessment and Retrofitting of Buildings. European Committee for Standardization: Bruxelles, Belgium, 2005.
70. Pinto, P.E.; Franchin, P. Eurocode 8—Part 3: Assessment and retrofitting of buildings. In Proceedings of the Eurocode 8 Background and Applications, Dissemination of Information for Training, Lisbon, Portugal, 10–11 February 2011.